Corrosion Science 77 (2013) 379-384

Effect of hydrogen on the surface energy of ferrite and austenite

Eun Ju Song [a] H. K. D. H. Bhadeshia [a,b] Dong-Woo Suh [a]

[a] *Graduate Institute of Ferrous Technology, POSTECH, Republic of Korea*

[b] *Department of Materials Science and Metallurgy, University of Cambridge, U.K.*

Abstract

Calculations indicate that the introduction of hydrogen into the body–centred cubic and face-centred cubic allotropes of iron in both cases reduces the {100} surface energy. The reduction is rather small in magnitude so this mechanism cannot present the major cause of the well–known hydrogen embrittlement phenomenon. Consistent with the theory of grain boundary embrittlement in iron, carbon is confirmed to increase the surface energy, thereby rendering cleavage fracture less likely assuming that other factors governing fracture are maintained constant.

Key words: hydrogen embrittlement, decohesion theory, first principles calculation, surface energy

1 Motivation

The embrittlement that occurs when small concentrations of hydrogen are introduced into body-centred cubic iron was first noted in 1875 [1]. The mechanisms postulated to explain this phenomenon include the internal pressure theory [2] where diffusible hydrogen accumulates at critical defects, combines to form molecular hydrogen and the resulting pressure helps initiate fracture. The second may involve a reduction in the cohesive energy of iron, thus making it easier to cleave [3]. In the localised plasticity model, hydrogen promotes dislocation mobility and if this happens in a localised region then it can result in a shear instability which in turn stimulates further failure modes such as cleavage [4].

Recently, Takano [5] investigated the cohesive energy in cleavage fracture on the {100} (cleavage) planes of single crystal α-iron with hydrogen occupying octahedral interstices. The fracture in the method was simulated by monitoring the energy change as the displacement of a {100} surface relative to the

underlying plane is increased. Decohesion is said to occur when the energy no longer changes with displacement. However, those calculations did not consider the lattice expansion due to the hydrogen addition into the octahedral interstices of ferrite; this can be seen from the fact that there was no increase in energy as the separation of {100} planes increase from 0 to 0.06 nm. So in this case, the energy reduction due to the hydrogen is overestimated. It was found that hydrogen reduced the cohesive energy, with the conclusion that it therefore assists crack initiation.

It is important to assess this conclusion again, taking account of the issues highlighted above, and in addition, accounting for the fact that hydrogen can occupy both the tetrahedral and octahedral interstices. The calculations have been conducted for austenite in addition to ferrite in order to provide a basis for comparison, and the role of carbon in influencing the surface energy is also examined. In the present work, the calculations were carried out for the case of hydrogen atoms; molecular hydrogen is not addressed, and neither is intergranular failure, which has been the subject of previous investigations [6, for example].

2 Calculation procedure

Density functional theory (DFT) [7,8] calculations were carried out with the Vienna ab initio simulation package commonly referred to as VASP [9–11] using the projector augmented wave basis set [12] and the generalized gradient approximation (GGA) of the Perdew, Burke, and Ernzerhof (PBE) form for electron exchange and correlation [13]. An energy cutoff of 450 eV was used for all calculations.

The ferrite was simulated using a $2 \times 2 \times 4$ supercell of conventional body-centred cubic structure with $6 \times 6 \times 3$ k–point sampling. For the austenite the supercell was $2 \times 2 \times 4$ of the conventional face-centred cubic structure with $8 \times 8 \times 4$ k–point sampling. Spin-polarised calculations were performed for ferrite and non-spin-polarised calculations in the case of austenite. Both cell shape and atomic positions were allowed to relax for bulk calculations. Lattice parameters of 2.84 and 3.45 Åwere obtained with ferrite and austenite, respectively. The reference hydrogen was assumed to be an H_2 molecule and the total energy of the hydrogen molecule was calculated by putting H_2 in a cubic box with 10 Å sides and carrying out a Γ–point calculation. A bond length of 0.75 Å was obtained for H_2.

For modelling the surface, the lattice parameters obtained from relaxed bulk Fe_n and Fe_nH were fixed and then the thickness of 0.2-10 Å vacuum layer was inserted. Only the atoms located in the top 5 layers were allowed to relax;

the bottom three layers were fixed at their bulk positions in order to maintain the vacuum between the layers undergoing separation during the simulation of cleavage. Same k–point samplings with the bulk metal were used for systems with vacuum thickness less than 10.0 Å, while $6 \times 6 \times 1$ and $8 \times 8 \times 1$ k–point samplings were used for ferrite and austenite respectively, for the systems with 10 Å thickness vacuum.

3 Results and discussion

3.1 H atoms in ferrite and austenite

Both octahedral and tetrahedral sites (Fig. 1) were investigated to assess the dissolution of hydrogen in the bulk matrix. Then the dissolution energy of hydrogen atoms in bulk Fe was obtained as follows, with the reference state of pure metal and H_2 molecule:

$$\Delta E_1 = E(\mathrm{Fe}_n\mathrm{H}) - E(\mathrm{Fe}_n) - \frac{1}{2}E(\mathrm{H}_2) \tag{1}$$

Here, n is the number of Fe atoms. Table 1 shows the dissolution energies (eV) of hydrogen in ferrite and austenite from the present study and together with data from the literature [14–16]. Our calculations are in reasonable agreement with reported data, and the discrepancy with reported experimental values comes from the zero-point energy [15,16]. [1] In ferrite, hydrogen is favoured at tetrahedral sites unlike the other interstitial atoms such as carbon and nitrogen. The results are in a good agreement with the literature [18–20]. For austenite, hydrogen is favoured at octahedral sites and its dissolution energy is smaller than in ferrite which explains the larger solubility of hydrogen in austenite than in ferrite. From equation 1, a positive ΔE_1 implies an increase in energy when hydrogen is dissolved. Note that a smaller ΔE_1 favours greater solubility.

The H-H interaction was investigated next, with the same supercell but including two hydrogen atoms. The interaction energy was studied as a function of the number of intermediate layers separating the two hydrogen atoms. For example, the ferrite atomic structures with two atoms are in Fig. 2. By analogy with equation 1, the dissolution energy ΔE was calculated as follows:

$$\Delta E_2 = \frac{E(\mathrm{Fe}_n\mathrm{H}_m) - E(\mathrm{Fe}_n) - m\frac{1}{2}E(\mathrm{H}_2)}{m} \tag{2}$$

[1] The zero point energy correction is usually negligible with heavy elements but for Fe-H system, large corrections have been reported [15,16]. Consistent with the present work, the correction is reported to be negligible for the Fe-C system [17]. The large difference in the case of the light atom hydrogen might be caused by the fact that the zero point energy has kinetic origins.

Here, m is the number of H atoms. It is evident from Table 2 that the dissolution energy increases as the distance between hydrogen atoms decreases, implying that the interaction between the two hydrogen atoms in ferrite and austenite lattice is repulsive. This result is somewhat surprising given that hydrogen is often said to combine within the steel to form voids, but such combinations are postulated to occur at defect sites where the thermodynamics must differ due to the existence of free surfaces or strain fields. There is unrelated evidence in chemisorption experiments on iron surfaces of specific repulsive interactions between hydrogen atoms [21] and from first principles calculations of adsorption on particular iron surfaces [22]. By studying the variation in dissolution energy as a function of hydrogen concentration (ΔE_1 are 0.2 eV, 0.16 eV, and 0.19 eV in Fe_2H, $Fe_{16}H$ and $Fe_{56}H$, respectively.) in ferrite, which is assumed to relate to a mean separation distance, Jiang and Carter [15] concluded that the variation was within numerical error (0.02 eV) and hence a H-H repulsion is non-existent. The numerical error in the present work is ± 0.0048 and ± 0.0070 eV, for ferrite and austenite respectively, given that k–point and cut off energy were chosen such that the energy difference is less than 0.00015 and 0.00011 eV per atom.

3.2 Effect of H on the {100} surface of ferrite and austenite

The vacuum thickness between the top (100) plane and the bulk, can be considered as a displacement, thus the increase in total energy is proportional to the force needed to implement this deformation. The atomic structures for modelling surface in pure metal are in Fig. 3. To see the effect of hydrogen, a hydrogen atom was added at tetrahedral and octahedral site for ferrite and austenite, respectively. Fig. 4. As an example, Fig. 5 shows the energy difference as a function of the vacuum thickness in the case of pure iron and when H atom is added at the tetrahedral site and octahedral site for ferrite and austenite, respectively. The results shows hydrogen reduces the force needed to deform. It is assumed that there is no interaction across the 10 Å thickness of vacuum. Similarly, calculations for H at octahedral and tetrahedral sites for ferrite and austenite were conducted and the dissolution energy ΔE_3 was calculated as follows:

$$\Delta E_3 = E(\mathrm{Fe}_n\mathrm{H} + \text{vacuum}) - E(\mathrm{Fe}_n + \text{vacuum}) - \frac{1}{2}E(\mathrm{H}_2) \tag{3}$$

The results are shown in Table 3. The dissolution energy hydrogen dramatically decreased for both ferrite and austenite. Also, for the ferrite, H atom prefers octahedral sites at the (100) surface unlike the bulk material [15,23]. From those results, the surface energy can be obtained as follows:

$$\Delta E_s = \frac{E(\mathrm{Fe}_n\mathrm{H} + \text{vacuum}) - E(\mathrm{Fe}_n\mathrm{H}_m)}{2\,A} \tag{4}$$

Here, n and m are the number of Fe and H atoms, respectively and A is the surface area. Note that the term $E(\mathrm{Fe}_n\mathrm{H}+\mathrm{vacuum})-E(\mathrm{Fe}_n\mathrm{H}_m)$ represents the energy difference between two supercells containing the same number of atoms, with $E(\mathrm{Fe}_n\mathrm{H}_m)$ representing the bulk and $E(\mathrm{Fe}_n\mathrm{H}+\mathrm{vacuum})$ the surface. The calculated surface energies for pure metal and hydrogen containing system for ferrite and austenite are indicated in Fig. 6. Both for ferrite and austenite, surface energy was reduced by adding a hydrogen. The stable positions of H at (100) surface are octahedral and tetrahedral sites for ferrite and austenite, respectively. The result is of the same order of magnitude as the reported binding energy of hydrogen to a hollow site at the (100) surface, which ranges from 0.78 [23] to 0.82 [24]. In this study, the value was 0.99, and the difference with reported data comes from the different H fractions at the surface and is discussed in detail in the next paragraph. The lowering of the surface energy by hydrogen decreases force needed to form new surfaces. This may explain a part of the reason why hydrogen embrittles iron, but it is noteworthy that the reduction in surface energy is quite small, just 7 % in the case of ferrite and 9 % for austenite. This is not sufficient to explain the well-established dramatic effect that hydrogen has on the toughness of ferritic steel. The fact that hydrogen similarly affects the surface energy of (100) austenite but does not exhibit pronounced embrittlement is not surprising because its flow stress is much less sensitive to temperature, and hence plastic flow occurs at a lower stress than that required to cause cleavage.

However, the extent of energy reduction is sensitive to the fraction of the surface covered by hydrogen atoms. There are 12 stable octahedral positions of H at the 2×2 supercell ferrite (100) surface. The "covering fraction" at the surface, Θ, can be defined as:

$$\Theta = \frac{\text{number of occupied sites}}{\text{total number of stable positions}} \tag{5}$$

It follows that Θ for ferrite is 0.083 since one H atom was placed at the surface. The surface energy of ferrite as function of Θ was calculated. The lattice parameter was optimised with H covered bulk and then this lattice parameter was used in the calculations associated with the H covered surface system. The lattice parameter change as a function of H covering-fraction is shown in Fig. 7. These results were obtained by comparing the energy of localised H bulk and that of the H covered surface are shown in Fig. 8. In the absence of the surface, the stable H concentration is very low, about 2.68×10^{-6} and 5.81×10^{-6} atomic % for ferrite and austenite, respectively [14]. Jiang and Carter [25] investigated the H effect on (110) surface of ferrite. They calculated {surface energy of pure iron / surface energy of H covered system}, $\gamma(\mathrm{H})/\gamma(0)$, as a function of H covering fractions. When one H atom was put at 2×2 supercell ferrite, $\gamma(\mathrm{H})/\gamma(0)$ was 0.90 while it is calculated as 0.96 in this study. They are of same order but the difference indicates that H effect is likely to be larger in (110) system. It should be noted that they

calculated the surface with the case that one H atom was placed at 2×2 supercell ferrite, and obtained the curve for various H covering fractions by decreasing the surface area. This led to an almost linear reduction of surface energy due to the increase of H covering fraction.

Even though the H solubility in pure iron is very small, we conducted surface energy calculations for large Θ because it is possible that during deformation, the surface could in principle attract hydrogen atoms from the bulk. However, when there is no surface, H atoms are very unlikely to segregate to a particular (100) plane inside the crystal. It follows therefore that in Eq. 4, the term $E(\mathrm{Fe}_n\mathrm{H}_m)$ can be susbstituted by $E^*(\mathrm{Fe}_n\mathrm{H}_m)$ so that the stable dissolution energy of hydrogen can remain 0.19 eV.

$$E^*(\mathrm{Fe}_n\mathrm{H}_m) = 0.19\,m + E(\mathrm{Fe}_n) + m\frac{1}{2}E(\mathrm{H}_2) \tag{6}$$

Here, all energies are in eV. The surface energy is then obtained by comparing the energy of unlocalized H in the bulk, and that at the covered surface (red line, Fig. 8). H reduces the surface energy and the amount of reduction increases with Θ.

In addition, the effect of carbon on the same surface energy was investigated. The obtained dissolution energy is shown in Table 4. Then the surface energy of the system with carbon in octahedral site was investigated by using same method. The results are shown in Fig. 9. Unlike the hydrogen, the carbon increases the surface energy. This result is consistent with grain boundary theory, where embrittlement is construed by comparing the energy of solutes at grain boundaries and free surfaces. Carbon is the only solute of many segregating species which enhances boundary cohesion [26,27] some of which is also based on first-principles calculations. This is because the increase in surface energy due to carbon outweighs the change in grain boundary energy. It therefore becomes unfavourable to expose boundaries. The influence of hydrogen is on the other hand detrimental [26]. It is speculated that when soluble carbon is present in iron, the influence of hydrogen on reducing the surface energy will be mitigated, especially if the presence of carbon does not have other detrimental effects such as through excessive strengthening.

In summary, the work presented here suggests that although hydrogen reduces the energy of the classical cleavage plane in ferrite, the effect is dependent on the fraction of the surface covered by hydrogen, so it may not be safe to attribute its embrittlement effect simply to changes in cohesive energy.

Acknowledgments: The authors are grateful for support from the POSCO Steel Innovation Programme, and to the World Class University Programme of the National Research Foundation of Korea, Ministry of Education, Science and Technology, project number R32–2008–000–10147–0.

References

[1] W. H. Johnson, On some remarkable changes produced in iron and steel by the action of hydrogen and acids, *Proceedings of the Royal Society of London*, 23 (1875) 168–179.

[2] C. A. Zapffe, Hydrogen embrittlement, internal stress and defects in steel. *Trans. AIME*, 145 (1941) 225–271.

[3] A. R. Troiano, Role of H and other interstitials in the mechanical behaviour of metals, *Trans. ASM*, 52 (1960) 54–80.

[4] C. D. Beachem, A new model for hydrogen-assisted cracking (hydrogen "embrittlement"), *Metallurgical Transactions*, 3 (1972) 437–451.

[5] N. Takano, First principles calculation of hydrogen embrittlement in iron, *Key Engineering Materials*, 417–418 (2010) 285–288.

[6] L. Zhong, R. Wu, A. J. Freeman, G. B. Olson, Charge transfer mechanism of hydrogen-induced intergranular embrittlement of iron. *Physical Reviews B*, 62 (2000) 13938–13941.

[7] P. Hohenberg, W. Kohn, Inhomogeneous electron gas, *Physical Reviews B*, 136 (1964) 864–871.

[8] W. Kohn, Time-dependent Kohn–Sham density-functional theory, *Physical Review A*, 1133 (1965) 140–148.

[9] G. Cresse, J. Hafner, Ab initio molecular dynamics for open-shell transition metals, *Physical Review B*, 47 (1993) (13115).

[10] G. Kresse, J. Furghmuller, Efficient iterative schemes for ab initio total-energy calculations using a plane-wave basis set, *Physical Review B*, 54 (1996) 11169.

[11] G. Kresse, J. Furghmuller, Efficiency of ab-initio total energy calculations for metals and semiconductors using a plane-wave basis set, *Computational Materials Science*, 6 (1966) 15–50.

[12] P. E. Blöchl, Projector augmented-wave method, *Physical Review B*, 50 (1994) 17953.

[13] J. P. Perdew, K. Burke, M. Ernzerhof, Generalized gradient approximation made simple, *Physical Review Letters*, 77 (1996) 3865–3868.

[14] F. D. Manchester ed., *Phase diagrams of binary hydrogen alloys*, volume 13. ASM International, Materials Park, Ohio, USA, 2000.

[15] D. E. Jiang, E. A. Carter, Diffusion of interstitial hydrogen into and through bcc Fe from first principles, *Physical Review B*, 70 (2004) 064102.

[16] W. A. Counts, C. Wolverton, R. Gibala, First-principles energetics of hydrogen traps in α-Fe, *Acta Materialia*, 58 (2010) 4730–4741.

[17] D. E. Jiang, E. A. Carter, Carbon dissolution and diffusion in ferrite and austenite from first principles, *Physical Review B*, 67 (2003) 214103.

[18] J. R. G. Da Silva, S .W. Stafford, R. B. McLellan, The thermodynamics of the hydrogen-iron system, *Journal of the Less Common Metals*, 49 (1976) 407–420.

[19] J. K. Nørskov, F. Besenbacher, J. Bøttiger, B.B. Nielsen, A. A Pisarev, Interaction of hydrogen with defects in metals: Interplay between theory and experiment, *Physical Review Letters*, 49(19) (1982) 1420–1423.

[20] A. Juan, R. Hoffmann, Hydrogen on the fe (110) surface and near bulk bcc fe vacancies: a comparative bonding study, *Surface science*, 421(1) (1999) 1–16.

[21] F. Bozso, G. Ertl, M. Grunze, M. Weiss, Chemisorption of hydrogen on iron surfaces, *Applications of Surface Science*, 1 (2003) 103–199.

[22] D. E. Jiang, E. A. Carter, Adsorption and diffusion energetics of hydrogen atoms on Fe (110) from first principles, *Surface Science*, 547 (2003) 85–98.

[23] A. Ramasubramanian, M. Itakura, E. A. Carter, Interatomic potentials for hydrogen in α-iron based on density functional theory, *Physical Review B*, 79 (2009) 174101.

[24] J Krueger, HD Kunze, E Schuermann, E Fromm, E Gebhardt, *Gas and carbon in metals*, Springer-Verlag, Berlin, 518–613, 1976.

[25] D. E. Jiang, E. A. Carter, First principles assessment of ideal fracture energies of materials with mobile impurities: implications for hydrogen embrittlement of metals, *Acta Materialia*, 52 (2004) 4801–4807.

[26] P. M. Anderson, J.-S. Wang, J. R. Rice, Thermodynamic and mechanical models of interfacial embrittlement, In G. B. Olson, M. Azrin, and E. S. Wright, editors, *Innovations in ultrahigh-strength steel technology*, US Army Materials Technology Laboratory, Massachusetts, USA, 1987.

[27] R. Wu, A. J. Freeman, G. B. Olson, Effects of carbon on Fe-grain boundary cohesion: first principles determination, *Physical Review B*, 53 (1996) 7504–7509.

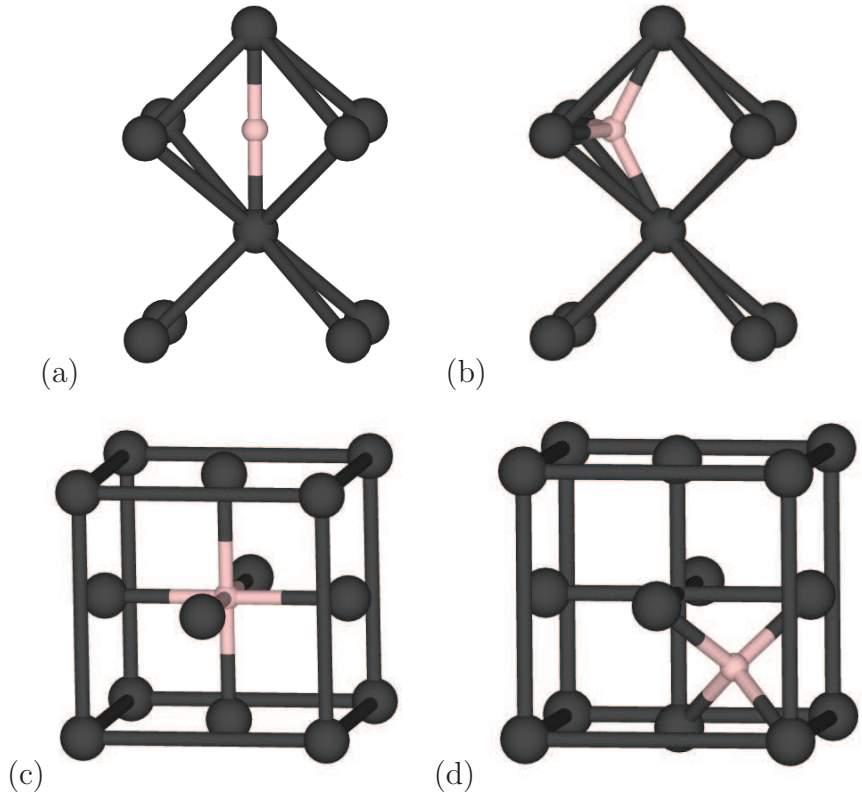

Fig. 1. Atomic structure for dissolution of hydrogen in (a) ferrite, octahedral (b) ferrite, tetrahedral (c) austenite, octahedral and (d) austenite, tetrahedral site, respectively.

Corrosion Science 77 (2013) 379-384

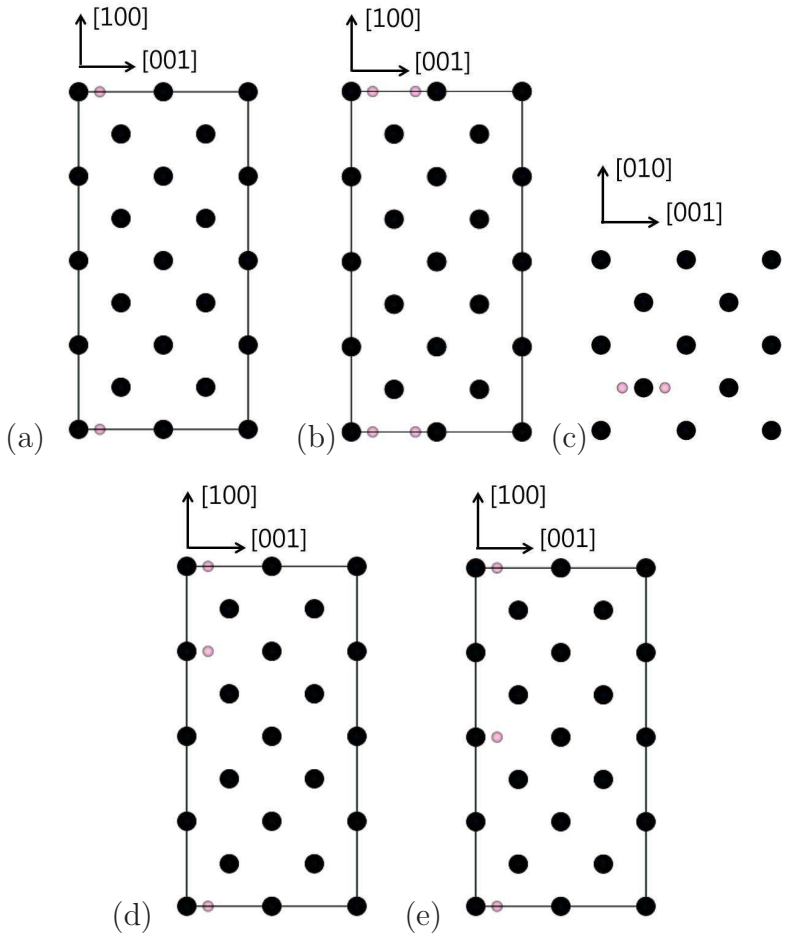

Fig. 2. Atomic structures for H–H interaction with different intermediate layers in ferrite (a) an atom, (b) two atoms with less than 1 intermediate layer (indicated as 0 intermediate layer in Table 2), (c) hydrogen configuration on (100) in the system (b), (d) 1 intermediate layer and (e) 3 intermediate layers

Table 1
Dissolution energy of hydrogen (eV) in ferromagnetic ferrite and non-magnetic austenite. The values in parenthesis are zero point energy corrected values.

Phase	Sites	Present work	Published calculated data	Measured data
ferrite	octahedral	0.34	0.32 [15], 0.34 [16]	–
	tetrahedral	0.19	0.19 (0.30) [15], 0.21 (0.30) [16]	0.30
austenite	octahedral	0.07	–	0.28
	tetrahedral	0.51	–	–

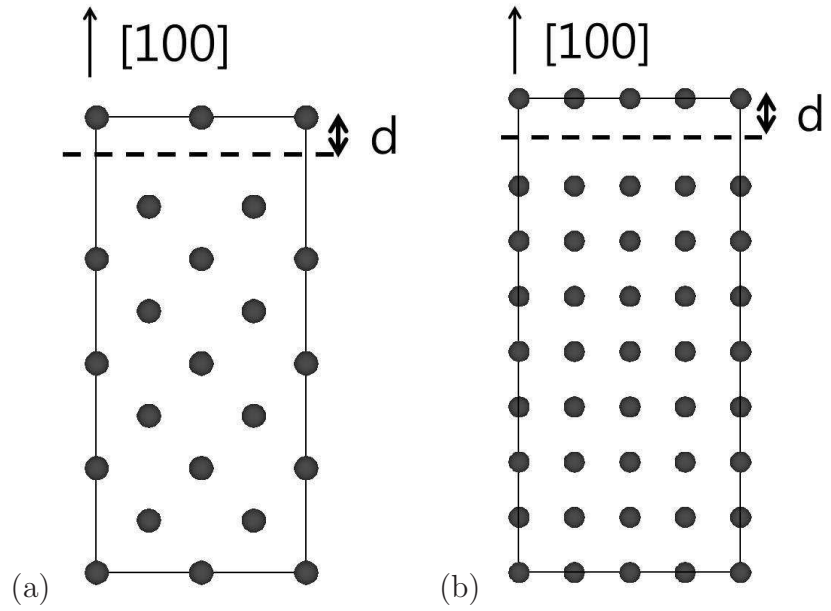

Fig. 3. Atomic structure for modelling the surface with d, vacuum distance of (a) ferrite (b) austenite

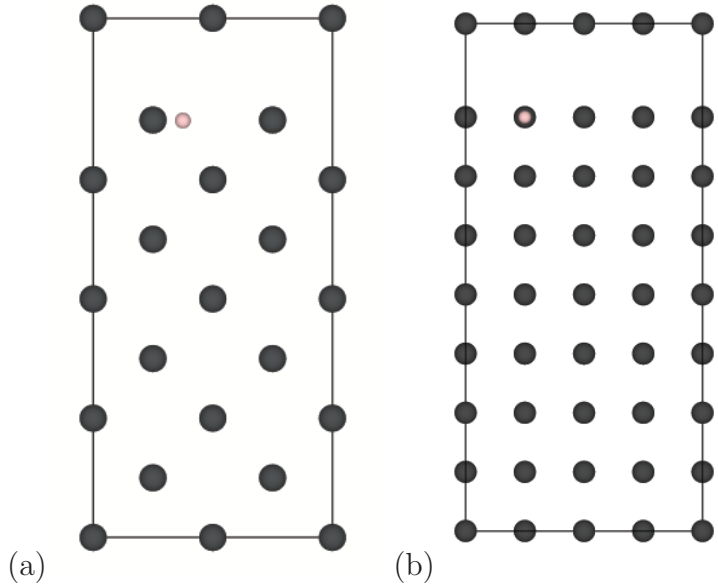

Fig. 4. Atomic structure for modelling the surface with hydrogen in (a) ferrite (b) austenite

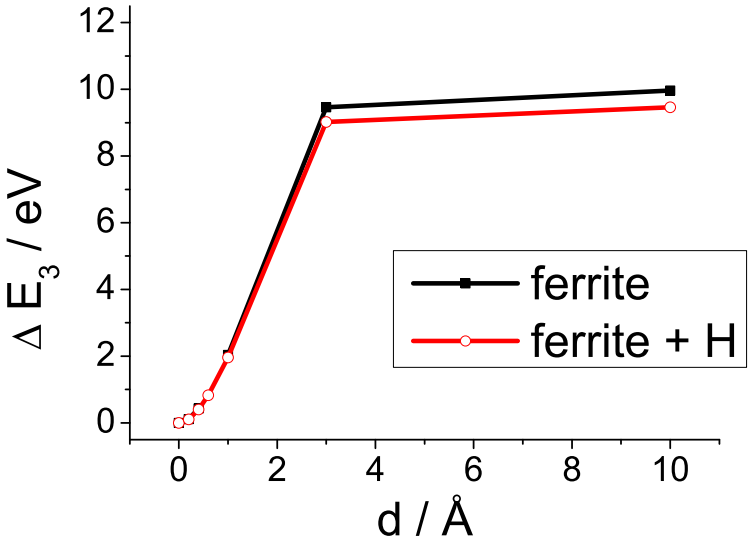

(a)

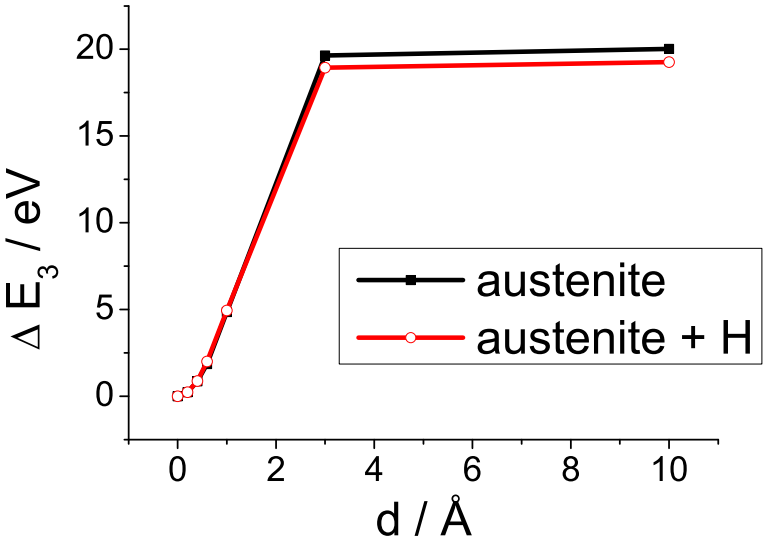

(b)

Fig. 5. The energy difference with d, vacumm distance of (a) ferrite (b) austenite for the pure iron and when H is added at a tetrahedral site and octahedral site, for ferrite and austenite, respectively

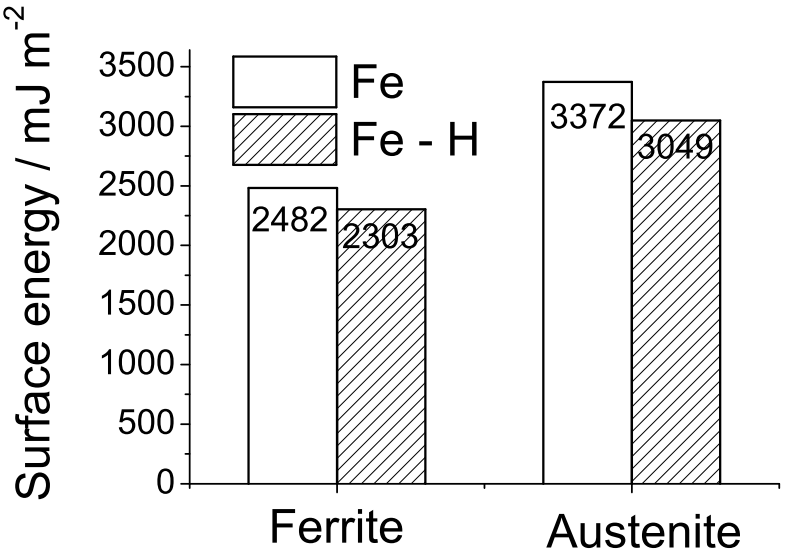

Fig. 6. The calculated surface energy of ferrite and austenite for pure metal and hydrogen containing system.

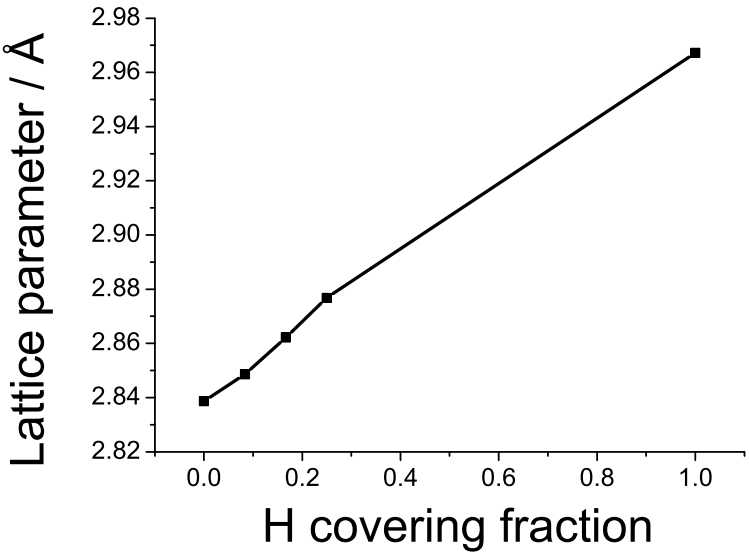

Fig. 7. The obtained lattice parameter as a function of H covering fractions

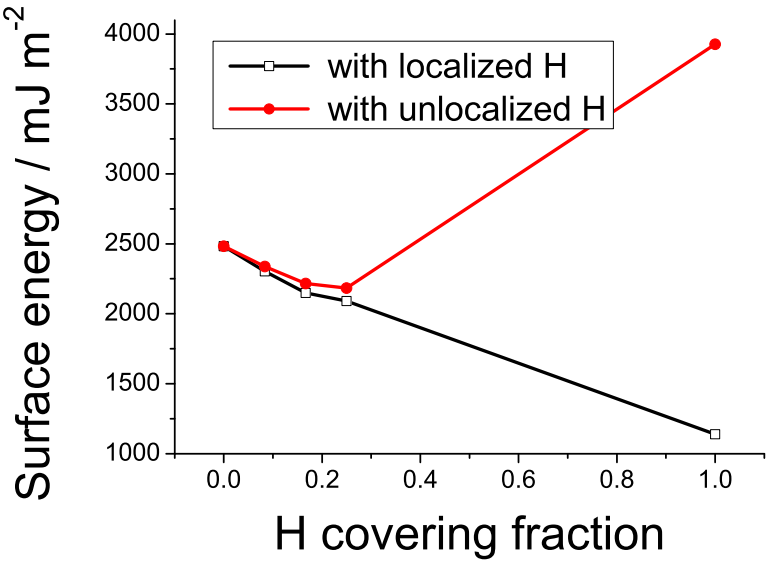

Fig. 8. The calculated surface energy of ferrite as a function of H covering fractions

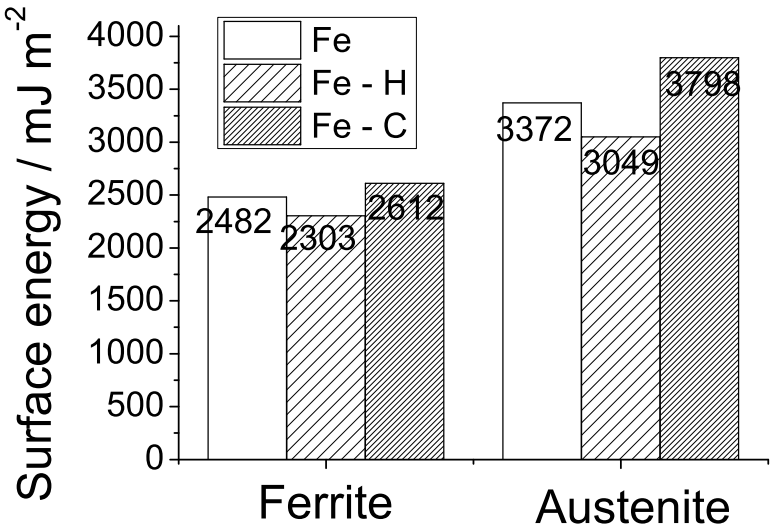

Fig. 9. The calculated surface energy of ferrite and austenite for pure metal and hydrogen, carbon containing system.

Table 2
Dissolution energy (eV) of hydrogen in ferrite and austenite as a function of the separation of two H atoms in units of the number of separating (100) planes

phase	single H atom	0 layer	1 layer	3 layers
ferrite	0.19	0.24	0.20	0.19
austenite	0.07	0.11	0.09	0.07

Table 3
Dissolution energy of hydrogen (eV) in ferromagnetic ferrite and non-magnetic austenite (100) surface.

Phase	Sites at bulk	Present work
ferrite	octahedral	-0.31
	tetrahedral	-0.29
austenite	octahedral	-0.38
	tetrahedral	-0.81

Table 4
Dissolution energy of carbon (eV) in ferromagnetic ferrite and non-magnetic austenite.

Phase	Sites	Present work
ferrite	octahedral	0.66
	tetrahedral	1.44
austenite	octahedral	-0.13
	tetrahedral	2.72